

# Smooth Gait Transition Based on CPG Network for A Quadruped Robot

Linlin Shang<sup>1,2</sup>, Zhaosheng Li<sup>1,2</sup>, Wei Wang<sup>1,2</sup>, and Jianqiang Yi<sup>1,2</sup>

**Abstract**— Aiming at achieving smooth gait transition for quadruped robots, we present a Hopf oscillator-based Central Pattern Generator (CPG) with controllable phase relationships in this paper. The proposed CPG controller can facilitate changing parameters to generate different locomotion gaits. Particularly, required phase relationships between every two oscillators can be obtained by modulating the duty factor and relative phases of legs. Therefore, smooth rhythmic signals for gait transition are generated. Moreover, the onset of the gait transition can be designed accurately. Finally, we verify the effectiveness of our controller on a simulated quadruped robot. Smooth and stable transition among walk, trot and pace gait has been achieved. Both transition from walk to trot and trot to pace are finished in a second.

## I. INTRODUCTION

After millions of natural selection and evolution, quadruped animals use multiple kinds of gaits and perform smooth gait transition among them to cope with locomotion speed change, reduce energy consumption and adapt to tough terrains [1]. This feature of such animals contributes to their superior stability and maneuverability to traverse various terrains. Inspired by quadruped locomotion, many quadruped robots [2]-[4] have been developed to conduct a series of adaptive locomotion experiments and execute various tasks in challenging environments. One typical example of quadruped robots for real-world application is ANYmal [5], which inspects machinery and infrastructure regularly and automatically on the offshore converter platform. However, few quadruped robots have the ability to outperform living creatures in terms of mobility and versatility.

For quadruped robots, the ability to generate different gaits and perform smooth gait transition is a fundamental requirement for completing useful tasks such as disaster rescue, search and detection. A flexible locomotion control model plays a decisive role in gait generation and gait transition for quadruped robots. Recently, research on locomotion control strategies using Central Pattern Generators (CPGs) for quadruped robots has made great progress. Such control systems, having advantage in robustness against perturbations and simple structure, can generate coordinated rhythmic signals for quadruped locomotion. A variety of quadruped gaits, including walk, trot, pace and gallop, are generated by CPGs and tested on both simulated and real quadruped robots [6]-[9]. H. Kimura et al. employ a CPG

network combined with a set of reflexes and responses, and perform successful adaptive walking tests on Tekken2 [6]. A CPG controller made up of four Hopf oscillators has been implemented on the quadruped robot “Cheetach” to generate walk gait [7]. Cheetah-cub achieves fast trotting gait under control of an open-loop CPG network [8]. Most of these control models focus on generation of one single gait pattern. However, quadruped robots have to freely change their gaits depending upon the terrain and speed in order to improve energy efficiency and keep stability.

Despite many excellent studies on gait transition, there are still challenges yet unsolved. Farhad Asadi et al. propose a Cartesian CPG-based controller and conduct simulations to validate its effectiveness [10]. This controller can achieve smooth gait transition by incorporating swing legs trajectories design into a CPG model. However, this approach requires exact knowledge about mechanical model of the robot. X. Q. Li achieve smooth and fast transition among walk, trot and gallop gait based on phase modulation [11]. However, the transition only occurs when the change rate of the oscillation is zero. X. L. Zhang achieves gait transition by directly modifying the gait matrix of CPGs [12]. This method is very simple, but control signals become discontinuous during transition.

To achieve stable and flexible locomotion, quadruped robots should change their gaits in a smooth and continuous way. Therefore, we present a Hopf oscillator-based CPG with controllable phase relationships. Motion trajectories of hip joints and knee joints are designed by setting phases of oscillators, and interlimb coordination is achieved by specifying phase relationships between oscillators. Smooth transition between different gaits can be easily achieved by gradual modulation of the duty factor and relative phases of legs. Moreover, the onset of the gait transition can be designed accurately. The gait transition approach is based on parameter modulation, so it is applicable to other quadruped models.

The remainder of the paper is organized as follows. An overview of quadruped gait patterns is described in Section II. In Section III, we introduce the Hopf oscillator-based CPG network with controllable phase relationships in detail. We firstly construct the CPG network by coupling four Hopf oscillators for gait generation. Then, we introduce the means to achieve transition from walk to trot and then to pace in detail. In Section IV, simulation are performed for validating the efficiency of the proposed approach. Finally, conclusions are given in Section V.

\*This work was supported in part by the National Natural Science Foundation of China under Grant 61375101.

<sup>1</sup>Institute of Automation, Chinese Academy of Sciences, 95 Zhongguancun East Road, Beijing, 100190, China.

<sup>2</sup>University of Chinese Academy of Sciences, 19A Yuquan Road, Beijing, 100049, China.

Corresponding author: Wei Wang, (wei.wang@ia.ac.cn)

## II. QUADRUPED GAIT PATTERN

Quadruped animals usually lift up their legs and touch down in a coordinated cyclic manner so that they can move forward with minimal energy consumption [13]. This manner, called a gait, plays a key role in keeping stability. Inspired by quadruped locomotion, quadruped robots perform several gaits to save energy, adapt to rough terrains and maintain stability. Typical quadruped gaits include walk, trot and pace gait.

Fig. 1 depicts phase diagrams of the walk, trot and pace gait [14]. As a statically stable gait, walk gait is characterized by having only one leg in the air. Walk gait has advantage in high stability, but the motion speed during walk gait is relatively low. Trot and pace gait, as dynamically stable gaits, are suitable when the motion speed is high and high energy efficiency is required. Diagonal legs of quadruped robots always swing synchronously during trot gait. Pace is the gait that ipsilateral legs of quadruped robots move in pairs.

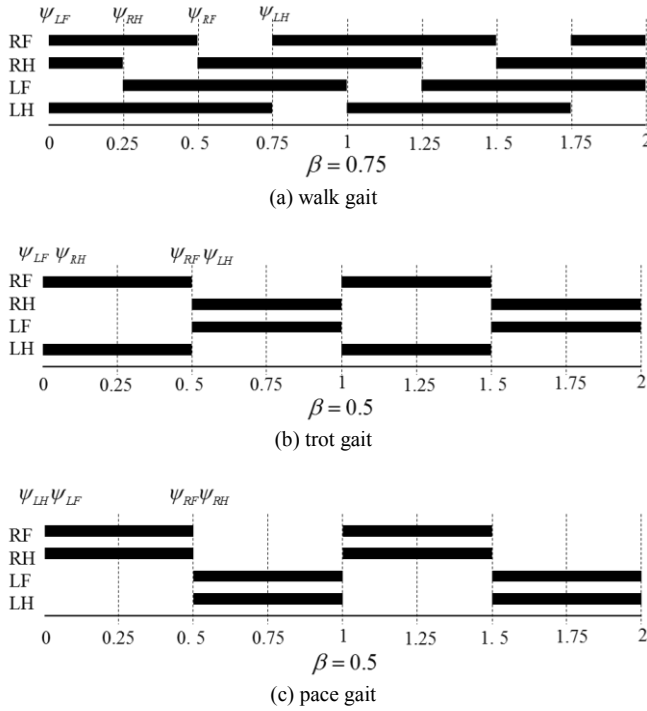


Fig. 1. Phase diagram of the walk, trot and pace gait. The blank block denotes swing phase, and the black block represents stance phase. LF, LH, RF and RH severally refers to left-fore leg, left-hind leg, right-fore leg and right-hind leg.  $\psi_{RF}, \psi_{RH}, \psi_{LF}, \psi_{LH}$  mean relative phases of RF, RH, LF and LH, respectively.  $\beta$  represents the duty factor. (a) Phase diagram of the walk gait. The swinging sequence of legs is LF-RH-RF-LH. (b) Phase diagram of the trot gait. The swinging sequence of legs is LF, RH-RF, LH. (c) Phase diagram of the pace gait. The swinging sequence of legs is LF, LH-RF, RH.

In these gait patterns, the duty factor  $\beta$  refers to the ratio of stance duration to one cycle period, defined as follows [15],

$$\beta = T_{st} / (T_{st} + T_{sw}) \quad (1)$$

where  $T_{st}$  is the duration of stance phase and  $T_{sw}$  is the duration of swing phase. The relative phases  $\psi_{RF}, \psi_{RH}, \psi_{LF}, \psi_{LH}$  indicate the swinging sequences of four legs. Quadruped gaits are classified by the order and timing of lifting legs and duration of stance and swing phases [16], i.e. the duty factor and relative phases of legs. Therefore, modulation of the duty factor and relative phases implies gait transition.

## III. HOPF OSCILLATOR-BASED CPG FOR GAIT TRANSITION

### A. Hopf Oscillator Model

The oscillator applied in our CPG model is the Hopf oscillator [17]. Compared to Matsuoka [18], Rayleigh [19] and Van der Pol oscillators [20], the Hopf oscillator has simpler structure and more stable model. Moreover, output signals of the Hopf oscillator can be easily modulated through limited parameters change. The mathematical expression of the Hopf oscillator is as follows:

$$\dot{x} = m(\mu - d^2)x - \omega y \quad (2)$$

$$\dot{y} = n(\mu - d^2)y + \omega x \quad (3)$$

$$\omega = \omega_{st} / (e^{-ax} + 1) + \omega_{sw} / (e^{ax} + 1) \quad (4)$$

$$d = \sqrt{x^2 + y^2} \quad (5)$$

where  $x$  and  $y$  are state variables of the oscillator.  $a$  is a positive constant.  $\mu$  determines the amplitude, and the oscillators stop oscillation when  $\mu$  is negative. The frequency of the oscillator is specified by  $\omega$  and it alters between two independent parameters:  $\omega_{st}$ , the frequency of the stance phase and  $\omega_{sw}$ , the frequency of the swing phase.  $m$  and  $n$ , as positive constants, specify the convergence velocity of  $x$  and  $y$  respectively.

As shown in Fig. 2, the Hopf oscillator has a structurally stable limit cycle, which provides robustness against transient perturbations. The limit cycle is globally stable, causing output signals to promptly return to its normal rhythmic cycle after temporary parameter tuning.

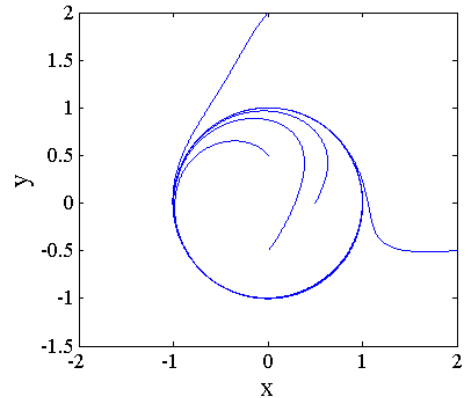


Fig. 2. An example of a limit cycle.

We prefer this choice of oscillator also because swing and stance frequencies can be independently controlled with  $\omega_{st}$  and  $\omega_{sw}$ . In Fig. 3, frequencies of the swing and stance phase are set to different values separately. When  $y > 0$ , the  $x$  trajectory is performing the stance phase. When  $y < 0$ , it is in swing phase. Duty factor  $\beta$  can be calculated as follows,

$$\beta = \frac{\omega_{sw}}{\omega_{sw} + \omega_{st}} \quad (6)$$

Thus, different gaits can be generated with desired duty factors.

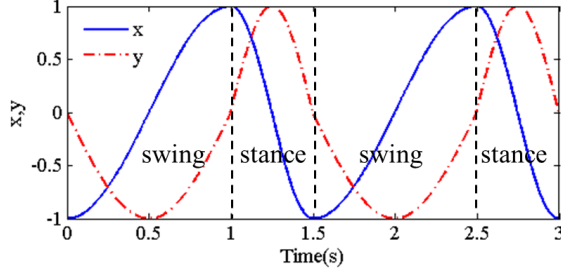


Fig. 3. Frequencies of swing and stance phases when setting  $\beta = 1/3$  and  $\omega_{st} = 2\omega_{sw}$ .

### B. CPG Network for Gait Generation

Different gaits have different interlimb coordination, i.e. relative phases among limbs. In our model, different interlimb coordination is achieved by coupling four Hopf oscillators with different phase relationships. The CPG network to generate fundamental gaits can be depicted by the equations [21]:

$$\dot{x}_i = m(\mu - r_i^2)x_i - \omega_i y_i + \sum_{j \neq i} (x_j \cos \theta_i^j - y_j \sin \theta_i^j) \quad (7)$$

$$\dot{y}_i = n(\mu - r_i^2)y_i + \omega_i x_i + \sum_{j \neq i} (y_j \sin \theta_i^j + x_j \cos \theta_i^j) \quad (8)$$

where  $x_i$  and  $y_i$  are two variables of  $i_{th}$  oscillator.  $i$  and  $j = 1, 2, 3, 4$  denote the index of each oscillator.  $\theta_i^j$  is the phase difference between the  $i_{th}$  and  $j_{th}$  oscillator.

In the CPG network, four coupled Hopf oscillators interact with each other to generate a series of stable rhythmic signals. Each oscillator is responsible for designing nominal trajectories of each limb.  $x_i$  corresponds to rotation angles of the hip joint.  $y_i$  is truncated as control signal of the knee joint to simplify the controller. Thus, the knee joint is defined such that it bends during swing phase and keeps motionless during stance phase. The specific phase relationships between every two oscillators result a gait. Therefore, the type of gaits is determined by  $\theta_i^j$  and the duty factor  $\beta$ , and we can achieve gait transition by modulation these parameters.

### C. Gait Transition

Quadruped gaits generated by the Hopf oscillator-based CPG network are described in terms of the duty factor and phase difference between every two oscillators. Therefore, gait transition can be realized through modulating these parameters. In this section, we introduce the gait transition approach through an example of walk-trot-pace transition.

Fig. 4 illustrates the phase difference between every two Hopf oscillators and relative phases for the walk, trot and pace gait, respectively. To achieve transition from walk to trot and then to pace gait, we select the phase of leg LH ( $\psi_3$ ) and leg RH ( $\psi_4$ ) as control variables. The phase relationships between oscillators are expressed in terms of functions of  $\psi_3$  and  $\psi_4$ , as listed in Table I. Therefore, we can obtain required phase relationships between every two oscillators corresponding to specified gait transition. Walk, trot and pace gait are generated successively by the Hopf oscillator-based CPG controller, along with modulation of the duty factor.

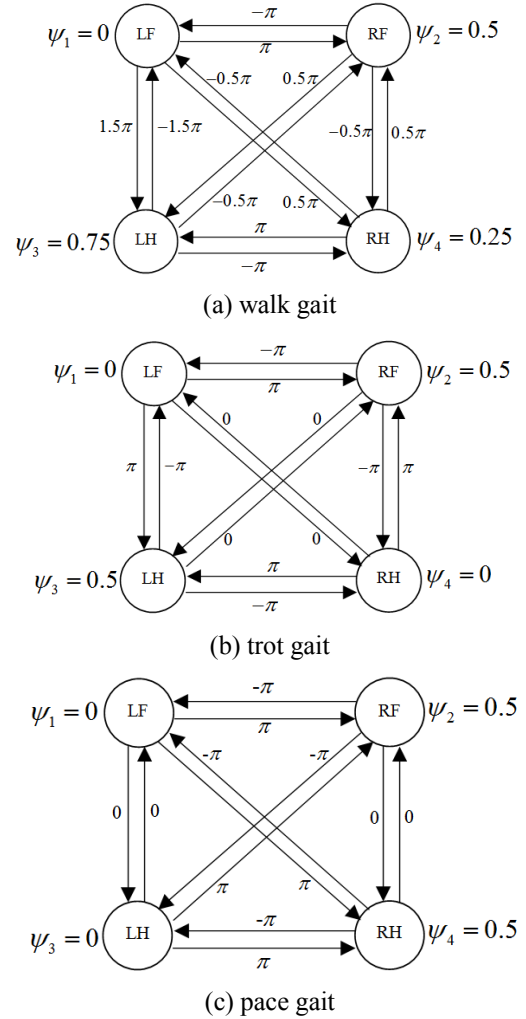


Fig. 4. Relative gait phases for legs and phase relationships between every two oscillators for walk, trot and pace gait.  $\psi_{RF}, \psi_{RH}, \psi_{LF}, \psi_{LH}$  are relative phases of RF, RH, LF and LH, respectively.  $\theta_i^j$ , marked above solid arrows, represent phase relationships between oscillators.

TABLE I.

PHASE RELATIONSHIPS  $\theta_i^j$  IN TERMS OF RELATIVE PHASES  $\psi_3, \psi_4$  AMONG WALK, TROT AND PACE GAIT

$i/j$	LF	RF	LH	RH
LF	0	$\pi$	$2\pi\psi_3$	$2\pi\psi_4$
RF	$-\pi$	0	$2\pi(\psi_3-0.5)$	$2\pi(\psi_4-0.5)$
LH	$-2\pi\psi_3$	$2\pi(0.5-\psi_3)$	0	$2\pi(\psi_4-\psi_3)$
RH	$-2\pi\psi_4$	$2\pi(0.5-\psi_4)$	$2\pi(\psi_3-\psi_4)$	0

In particular, abrupt modulation of motion trajectories may cause stumble and hinder robots during locomotion. Smooth gait transition is essential for locomotion stability. To transform gaits smoothly, the phase of leg LH ( $\psi_3$ ) and leg RH ( $\psi_4$ ) need to be adjusted continuously:

$$\beta = \begin{cases} 0.75, & t < t_{wt} \\ 0.75 - 0.25(t - t_{wt}) / w_{wt}, & t_{wt} \leq t \leq t_{wt} + w_{wt} \\ 0.5, & t > t_{wt} + w_{wt} \end{cases} \quad (9)$$

$$\psi_3 = \begin{cases} \beta, & t < t_{tp} \\ \beta - 0.5(t - t_{tp}) / w_{tp}, & t_{tp} \leq t \leq t_{tp} + w_{tp} \\ \beta - 0.5, & t > t_{tp} + w_{tp} \end{cases} \quad (10)$$

$$\psi_4 = 2\beta - \psi_3 - 0.5 \quad (11)$$

where  $\beta$  is the duty factor.  $\psi_3$  and  $\psi_4$  are the gait phases of LH and RH, respectively.  $t_{wt}$  and  $t_{tp}$  is the start time of walk-trot transition and trot-pace transition, respectively.  $w_{wt}$  and  $w_{tp}$  represent the lasting time of walk-to-trot transition and trot-to-pace transition, respectively.

In the whole process, the quadruped robot starts in walk gait. Then it begins to transit to trot at  $t_{wt}$  and finishes at  $t_{wt} + w_{wt}$ . In the meantime, the duty factor and the gait phase  $\psi_3$  linearly reduces from 0.75 to 0.5, and the gait phase  $\psi_4$  linearly decreases from 0.25 to 0. Next, the second modulation for gait phases  $\psi_3$  and  $\psi_4$  occurs at  $t_{tp}$ . It takes  $w_{tp}$  to form the new phase coordination, while the duty factor keeps 0.5 during this time. This modulation leads to gait transition from trot to pace. As a result, the gait transition has been completed smoothly. Moreover, the onset of the gait transition can be designed accurately by setting values of  $t_{wt}$  and  $t_{tp}$ .

#### IV. SIMULATION AND DISCUSSION

##### A. Simulated Quadruped Robot

A simulated quadruped robot, as shown in Fig. 5, is built in MD Adams 2013 to validate the effectiveness of the proposed controller. This simulated model is composed of a torso and four legs. Each leg, composed of a thigh, shank and foot, has

two degrees of freedom, a hip pitch joint and knee pitch joint. This model is 1.05 m long, 0.72 m wide and 0.66 m high. A total weight of the quadruped model is about 50.0 kg. More detailed parameters of the simulated robot are shown in Table II.

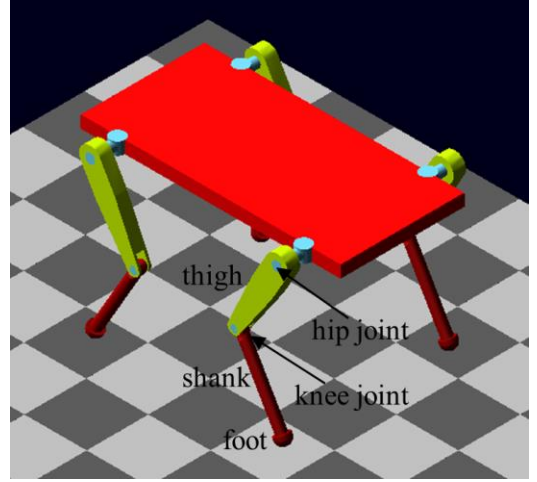


Fig. 5. The simulated quadruped robot.

TABLE II.

PARAMETER OF SIMULATED QUADRUPED ROBOT

Part	Volume ( $mm^3$ )	Density ( $kg/mm^3$ )	Mass (kg)	X-inertia ( $kg \cdot mm^2$ )
Torso	2.595E+007	7.707E-007	20	2.234E+006
Hip-link	2.500E+005	5.892E-006	1.5	2554.058
Thigh	1.411E+006	3.023E-006	3.5	3.763E+004
Shank	4.327E+005	4.662E-006	2.0	2.035E+004
Foot	8.482E+004	5.894E-006	0.5	195.012

##### B. Simulation Results and Analysis

The proposed controller is tested on the simulated robot to perform walk, trot and pace gait successively. Control signals generated by the CPG controller, related parameters and the velocity of the robot are shown in Fig. 6. Fig. 7 depicts nine representative snapshots from the simulation video. In Fig. 6, the duty factor  $\beta$  of walk gait is 0.75, and the duty factor of trot and pace gait is 0.5, as plotted in the first frame. The curves in the second frame show the modulation of the LH leg gait phase  $\psi_3$  in blue and the RH leg gait phase  $\psi_4$  in black, respectively.

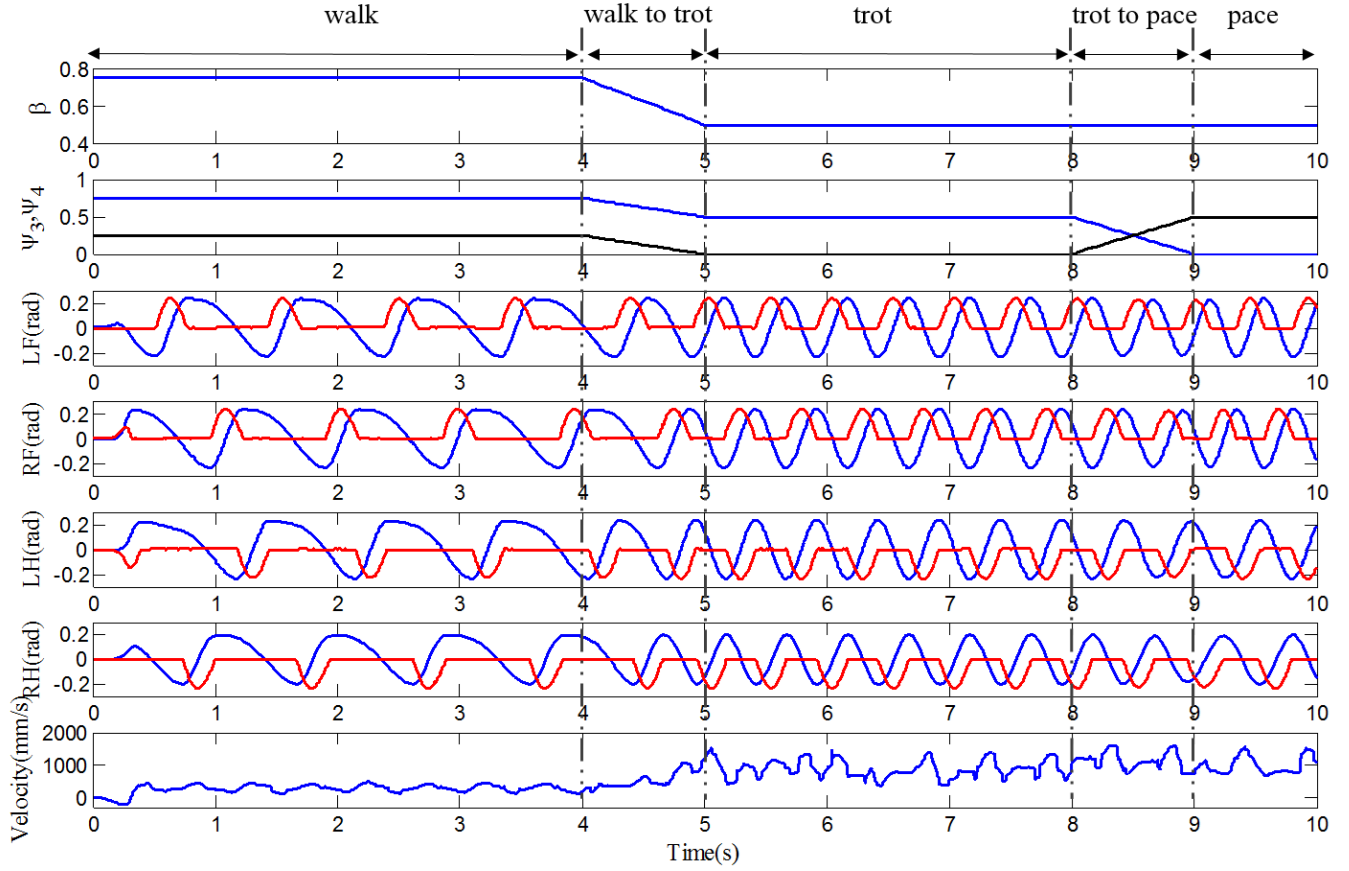


Fig. 6. Modified parameters, control signals and locomotion speed fluctuation during walk-trot-pace transition. The black line on the second frame is the phase of leg LH ( $\psi_3$ ) and the blue line is the phase of leg RH ( $\psi_4$ ). The resulting control signals of leg LF, RF, LH, RH are plotted in the third, fourth, fifth and sixth frame, respectively. The blue lines are signals for hip joints and the red ones are for knee joints. Bottom frame depicts the speed fluctuation during locomotion.

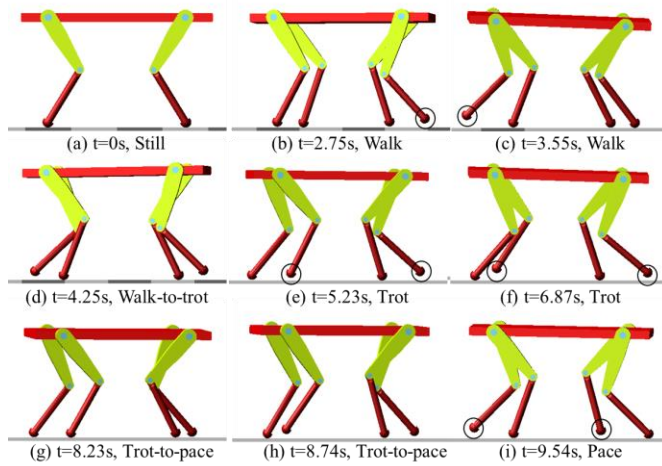


Fig. 7. Snapshots of simulation. The black circles represent the legs in swing phases.

The walk-to-trot transition is completed by linearly reducing the values of  $\beta$ ,  $\psi_3$  and  $\psi_4$ . At the meanwhile, the locomotion period changes from 1 second to 0.5 second. This transition starts at 4 s and takes one second. The quadruped robot trots from 5 s to 8 s. And then the transition from trot to

pace is achieved at 9 s. The frames from the third to sixth depict the control signals. Blue solid lines correspond to control signals for hip joints, while the red ones are for knee joints.

The bottom frame show the fluctuation of the locomotion speed during the simulation. The mean velocity during walk gait is 505 mm/s, and the standard deviation is 40 mm/s. Then, the robot accelerates to around 1000 mm/s as the gait transforms to trot, with a standard deviation of 80mm/s. The robot begins to pace at 9 s and it has an average velocity of 1125 mm/s with a standard deviation is 130 mm/s. Moreover, the locomotion speed of trot and pace gait fluctuates in a larger range than walk gait. It makes sense since trot and pace gait are dynamically stable and walk gait is statically stable.

Fig. 7 (a) shows initial posture of the simulated quadruped robot. In Fig. 7 (b)-(c), it starts to walk with three legs supporting the torso simultaneously. Then the robot begins to move the diagonal legs in pairs and its gait evolves to trot. In Fig. 7 (g)-(h), the trot gait transforms to pace gait. In Fig. 7 (i), the LF leg and LH leg lift off the ground while the others touch on the ground. During the whole transition, the torso maintains stable since there is no apparent fluctuation.

The ground reaction force (GRF) is detected for further evaluation of locomotion stability and smoothness. In this research, we regard the vertical components of the GRF as foot-ground contact force for the sake of convenience. This



force experienced by RF is shown in Fig. 8. During walk gait, the foot-ground contact force is about 0.25 kN, which is close to half of the total weight. The force becomes two times larger during the trot and pace gait. The peak value of the foot-ground contact force during the walk gait is below 1 kN, and larger in trot and gait pace gait, which is less than 1.6 kN. In a word, most of the foot-ground contact force experienced by RF is regular and in reasonable range during simulation. Moreover, RF in swing phase is off the ground and RF in stance phase is in contact with the ground in most of the time. This suggests the gait transition is stable and smooth.

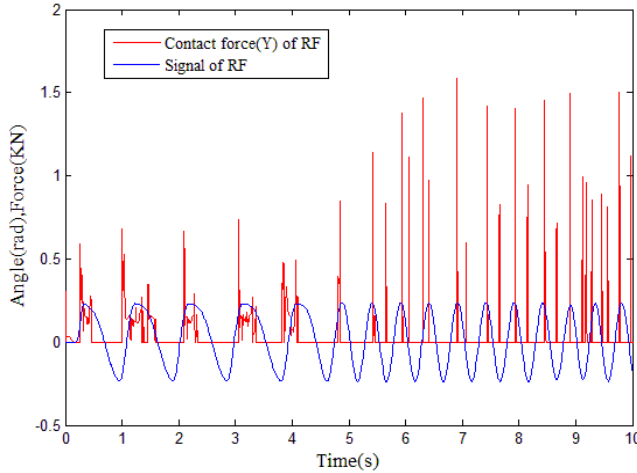


Fig. 8. Control signal for hip joint and contact force of RF limb.

## V. CONCLUSION

In this contribution, we propose a Hopf oscillator-based CPG controller with controllable phase relationships to achieve smooth gait transition for quadruped robots. This controller utilizes a CPG network modeled as four coupled Hopf oscillators as basis. In particular, we linearly increase or decrease the duty factor and relative phases of legs to satisfy the phase relationships between oscillators of the required gait. As a result, the controller generates continuous rhythmic signals for gait transition among three gaits. Using the proposed controller, the simulated model perform gait transition from walk to trot and then to pace successfully. The smoothness and stability of the proposed gait transition approach is validated by analyzing the speed fluctuation and foot-ground contact force experienced by RF. The proposed approach for gait transition fully depends on parameter modulation. It can be easily used for gait transition between any other gaits and other quadruped models.

Future work will be aimed at implementing this controller on a real quadruped robot developed in our lab.

## REFERENCES

- [1] R. M. Alexander, Principle of animal locomotion. Princeton: Princeton University Press, 2003.
- [2] M. Raibert, K. Blankespoor, G. Nelson, R. Playter, and the BigDog Team, "BigDog, the rough-terrain quadruped robot," in *17th World*

- Congress on the International Federation of Automatic Control*, pp. 10822-10825, 2008.
- [3] M. Kalakrishnan, J. Buchli, P. Pastor, M. Mistry, and S. Schaal, "Learning, planning, and control for quadruped locomotion over challenging terrain," *The International Journal of Robotics Research*, vol. 30, no. 2, pp. 236-258, 2011.
- [4] I. M. Koo, D. T. Tran and Y. H. Lee et al, "Development of a quadruped walking robot AiDIN-III using biologically inspired kinematic analysis," *International Journal of Control, Automation and Systems*, vol. 11, no. 6, pp. 1276-1289, 2013.
- [5] M. Hutter, C. Gehring and A. Lauber et al, "ANYmal - toward legged robots for harsh environments," *Advanced Robotics*, 2017:1-14.
- [6] H. Kimura and Y. Fukuoka, "Biologically inspired adaptive dynamic walking in outdoor environment using a self-contained quadruped robot: 'Tekken2'," *Proc. of IEEE/RSJ International Conference on Intelligent Robots and Systems and Systems*, pp. 986-991, 2004.
- [7] S. Rutishauser, A. Sprowitz, L. Righetti, et al. "Passive compliant quadruped robot using central pattern generators for locomotion control," in *Proceedings of the 2nd International Conference on Biomedical Robotics and Biomechanics*, Scottsdale, USA, pp. 19-22, 2008.
- [8] A. Sprowitz, A. Tuleu, M. Vespignani, M. Ajallooeian, E. Badri, and A. J. Ijspeert, "Towards dynamic trot gait locomotion: Design, control, and experiments with Cheetah-cub, a compliant quadruped robot," *The International Journal of Robotics Research*, 2013.
- [9] M. Ajallooeian, S. Pouya, A. Sprowitz, et al. "Central Pattern Generators augmented with virtual model control for quadruped rough terrain locomotion," in *IEEE International Conference on Robotics and Automation*, pp. 3321 - 3328, 2013.
- [10] Asadi, Farhad, M. Khorram, and S. A. A. Moosavian, "CPG-based gait transition of a quadruped robot," *IEEE/RSI International Conference on Robotics and Mechatronics (ICROM)*, 2015.
- [11] X. Li, W. Wang, and J. Yi, "Gait Transition Based on CPG Modulation for Quadruped Locomotion," in *IEEE/ASME International Conference on Advanced Intelligent Mechatronics*, pp. 500-505, 2015.
- [12] X. L. Zhang, "Biological-inspired rhythmic motion and environmental adaptability for quadruped robot," Ph.D. dissertation, Tsinghua University, Beijing, China, 2004.
- [13] T. M. Griffin, R. Kram, S. J. Wickler, and D. F. Hoyt, "Biomechanical and energetic determinants of the walk-trot transition in horses," *Journal of Experimental Biology*, vol. 207, no. 24, pp. 4215-4223, 2004.
- [14] M. Hildebrand, "Symmetrical gaits of horses," *Science*, 150, 701-708, 1965.
- [15] K. Inagaki and H. Kobayashi, "A gait transition for quadruped walking machine," In *Proceeding on IEEE/RSJ international conference on intelligent robots and systems*, pp. 525-531, 1993.
- [16] R. B. Mcghee and A. A. Frank, "On the stability properties of quadruped creeping gaits," *Mathematical Biosciences*, vol. 3, pp. 331-351, August 1968.
- [17] C. Santos, and V. Matos, "Gait transition and modulation in a quadruped robot: A brainstem-like modulation approach," *Robotics and Autonomous Systems*, vol. 59, no. 9, pp. 620-634, 2011.
- [18] H. Kimura and Y. Fukuoka, "Biologically inspired adaptive dynamic walking in outdoor environment using a self-contained quadruped robot: 'Tekken2'," *Proc. of IEEE/RSJ International Conference on Intelligent Robots and Systems and Systems*, pp. 986-991, 2004.
- [19] A. C. de Pina Filho, M. S. Dutra, and L. S. Raptopoulos, "Modeling of a bipedal robot using mutually coupled Rayleigh oscillators," *Biological Cybernetics*, vol. 92, no. 1, pp. 1-7, 2005.
- [20] M. S. Dutra, A. C. de Pina Filho, and V. F. Romano, "Modeling of a bipedal locomotor using coupled nonlinear oscillators of Van der Pol," *Biological Cybernetics*, vol. 88, no. 4, pp. 286-292, 2003.
- [21] V. Matos, C. Santos, and C. Pinto, "A brainstem-like modulation approach for gait transition in a quadruped robot," in *IEEE International Conference on Intelligent Robots and Systems*, pp. 2665-2670, 2009.